



Recent advances in electrospray sampling efficiency and implications for LC-MS

Leigh Bedford, Bradley B. Schneider, Hassan Javaheri, Thomas R. Covey
SCIEX, 71 Four Valley Drive, Concord, ON, L4K 4V8 Canada

ABSTRACT & INTRODUCTION

Sampling efficiency, defined as the ratio of the number of ions captured in the first vacuum stage of the entrance optics to the number of analyte molecules entering the ion source, is a measure of sensitivity that takes into account both ionization efficiency at atmospheric pressure, the efficiency of transporting the ions from atmosphere to vacuum, and the efficiency of confining them in the subsequent gas expansion before mass analysis. Sampling efficiency measurements were conducted under high-performance liquid chromatography sample introduction conditions using columns and flow rates spanning the nanoflow (300 nL/min), microflow (3–60 µL/min), and milliflow (100–500 µL/min) ranges. The results show a convergence in the sampling efficiencies across this range, narrowing the sensitivity gap between the nanoflow and higher flow rate ranges largely because nanoflow sampling efficiency has been shown to be close to 100% for more than a decade, leaving little room for improvement. Under situations where sample volumes are not limiting, lower concentration detection limits can now be achieved with the higher flow rate systems versus nanoflow as a direct consequence of the higher sample loading capacity of the columns and the reduction in the difference in their ion sampling efficiencies.

MATERIALS AND METHODS

Sample preparation:

For infusion experiments, reserpine standards (from Sigma-Aldrich Co.) were diluted to 1 pg/µL in a solvent mixture comprising approximately 2:5:3:1 ethanol, methanol, water, and isopropyl alcohol with 0.1% formic acid. For LC experiments, reserpine standards were prepared in water with 0.1% formic acid. Bovine serum albumin (BSA, Sigma-Aldrich Co.) was trypsin-digested following a standard procedure [1] to produce stock solutions containing 30 pmol/µL of digested BSA, which were frozen at -20° C in aliquots. Prior to analysis, each BSA stock was diluted to 1 fmol/µL in solvent comprising water with 0.1% formic acid.

HPLC conditions:

The nanoLC-MS experiments were conducted using a nanoLC 400 system (SCIEX) operated in direct injection configuration with the use of a commercial packed emitter (New Objectives Inc., PF7510-150H354-3P). High flow experiments and LC splitting experiments were conducted using a Shimadzu Prominence XR LC system. For the LC splitting experiments, the column diameter was 2.1 mm. For the experiments without flow splitting, the column diameters were 75 µm, 300 µm, and 2.1 mm for LC experiments at 300 nL/min, 3 µL/min, and 200µL/min, respectively. Split ratios were measured gravimetrically in triplicate to ensure accuracy. Details of the tubing dimensions used to obtain the desired split ratios are provided in Table 1.

desired liquid flow rate (µL/min)	split capillary i.d. (µm)	split capillary length (cm)	measured flow rate (µL/min)
500	N/A	N/A	495.3
250	50	44.5	253.38
120	50	13.75	117.35
60	75	32.1	64.42
20	75	11	24.89
5	150	35.2	5.15

Table 1. Tubing dimensions for split flow LC-MS experiments

MS/MS conditions:

Experiments were conducted on a QTRAP 6500+ system. For experiments in the nanoflow regime, the standard curtain chamber was replaced with a nanoflow ESI compatible configuration that included a heated laminar flow chamber with a 2 mm inner diameter. The gas throughput on this system was approximately 4 L/min, and there were two stages of differentially pumped vacuum system prior to the high vacuum chamber containing the mass analyzers. The two differentially pumped vacuum chambers included quadrupole ion guides with typical operating pressures of approximately 2 Torr and 7 mTorr as previously described. For some experiments, the inlet configuration was modified to increase the gas throughput to approximately 16 L/min. For these experiments, the orifice diameter was drilled out, and an additional differentially pumped vacuum stage was installed between the inlet orifice and the stage containing the first quadrupole ion guide. The additional vacuum stage was pumped to approximately 6 Torr and included a custom dodecapole ion guide which has been described previously [2]. A prototype nanoflow interface was designed in-house to optimize performance for nanoflow ESI with a 16 L/min gas throughput. On both systems, data were acquired in multiple reaction monitoring (MRM) mode.

RESULTS

A modification of the high gas throughput interface was made to adapt to nanoflow operation by designing a large bore heated laminar flow chamber [3] that was sealed to the inlet, as is shown in Figure 1.

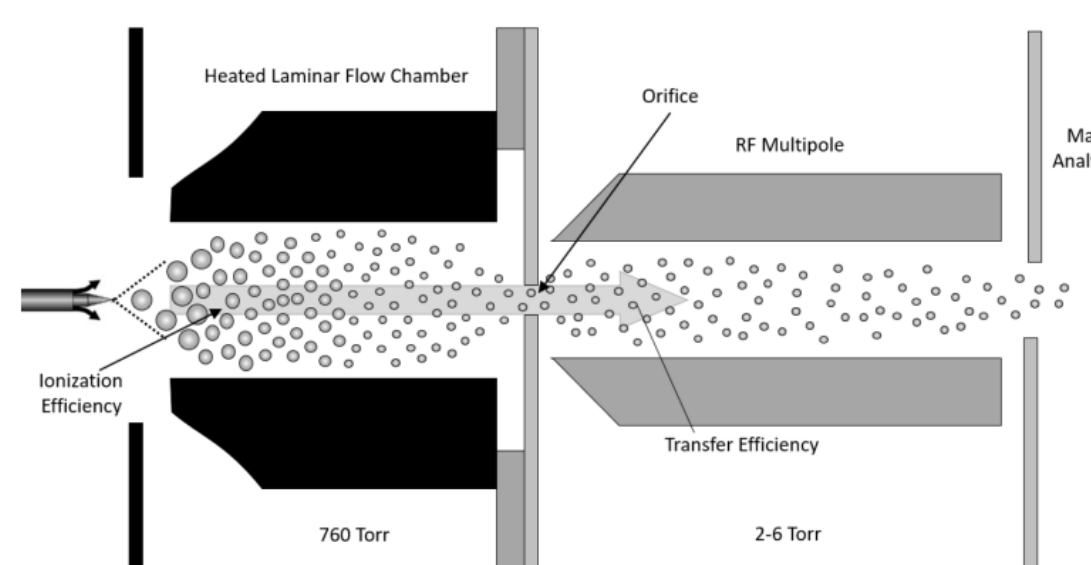


Figure 1. Nanoflow ESI interface design for the new high-throughput instrument. The inlet orifice (labeled orifice) diameter was 1.5 mm, and the first vacuum stage included a dodecapole ion guide (labeled RF multipole). The nanoflow interface included a heated laminar flow chamber sealed to the inlet orifice. The laminar flow chamber was approximately 1 cm long and included a 4.5 mm internal channel diameter.

The laminar flow chamber included a heater to control the temperature up to approximately 250° C. Signal intensity was relatively insensitive to both sprayer position and ion spray potential, as shown in Figure 2, where the maximum signal was measured within approximately ± 1 mm of the centerline of the heated inlet, with an applied potential of 3000 ± 500 V. When the sprayer was 2 mm off center from the bore of the laminar flow chamber, only about 50% of the nanoflow ESI plume overlapped effectively with the sampling inlet, and as expected, the signal intensity dropped by a factor of 2. The data from this optimization experiment roughly define the cross-sectional area of the region in the ion source from which ions are drawn in by the vacuum system as being approximately 4 mm² using the large bore sampling chamber. Ions that are not introduced directly into this region can be lost to various surfaces in the source or interface region as is the case with the majority of ions created with inlet fluid flows greater than nanoflow ESI. As the vacuum draw increases with larger apertures and vacuum pumps, the region where ions are sampled increases, and this improves the sampling efficiency.

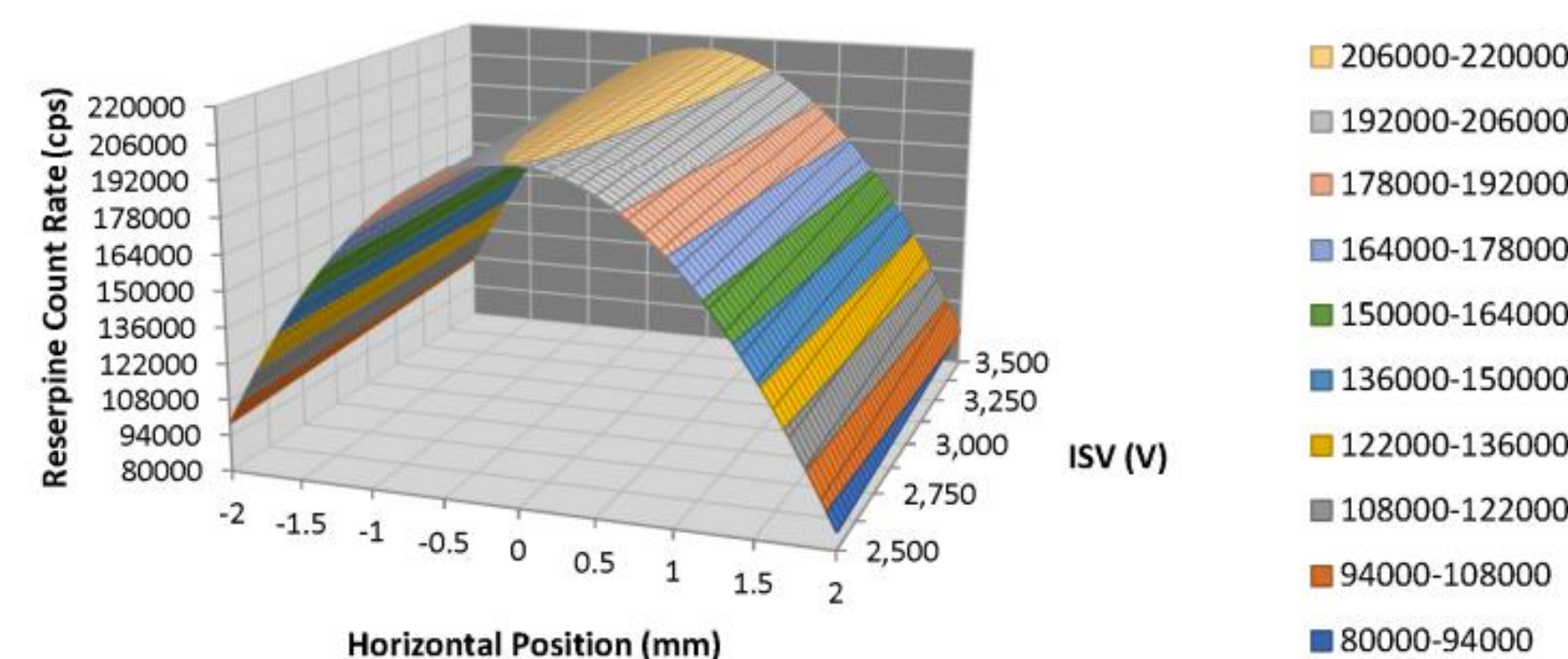


Figure 2. Surface plot of reserpine signal intensity as a function of horizontal position relative to the inlet of the mass spectrometer and ionization voltage. Data were acquired using a 3-level, 3-factor "Design of Experiments" (DOE) (SigmaZone, Quantum XL 2013), where a total of 27 runs were conducted with different combinations of sprayer radial position, ion spray potential, and nebulizer gas flow. Transmission was measured by monitoring the signal for reserpine ions using a fully articulated ion source to permit positional adjustment and the experiments were replicated three times. The results were independent of whether the radial position was adjusted horizontally or vertically. The validity of the model was verified with eight verification runs at the midpoint values for the tested parameters. The experimental values matched the model predictions to within 10% in all cases.

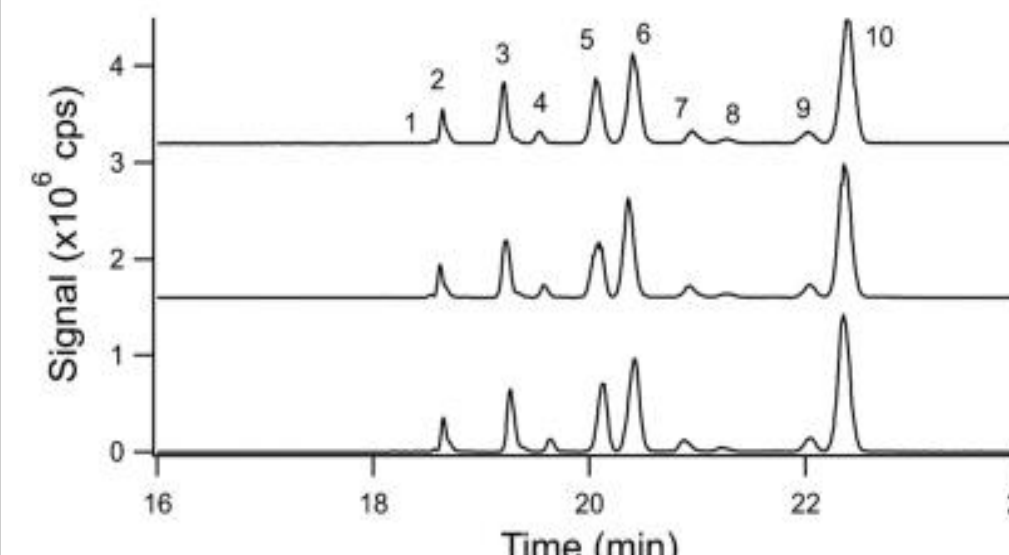


Figure 3A. Replicate nanoflow LC-MS data for MRM analysis of 10 peptides from a BSA digest. Typical CV's for these peptides were on the order of 3.95% for N=6 injections

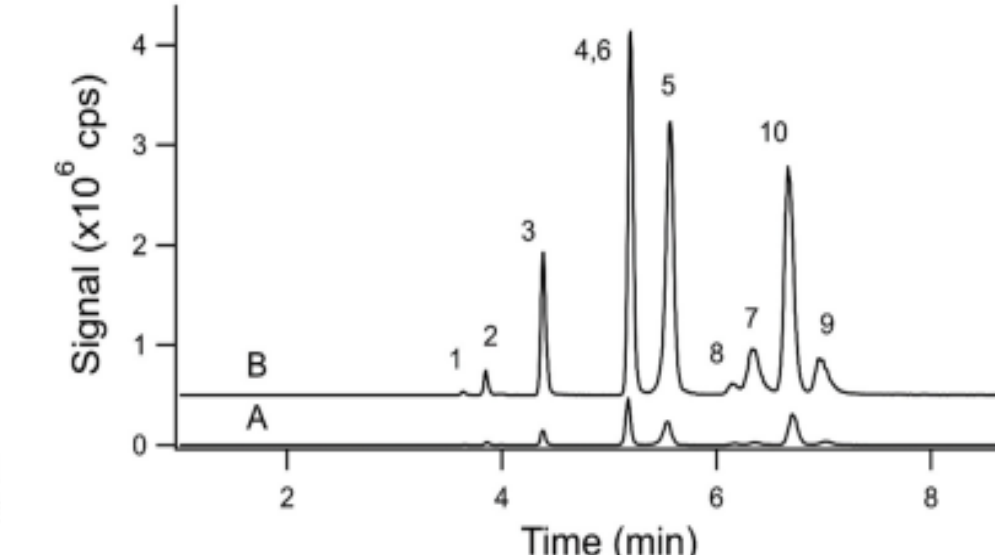


Figure 3B. Microflow LC-MS data taken at 3 µL/min flow rate with a 1 µL injection (A) and a 10 µL injection (B)

Prior to starting the split flow experiments to determine sampling efficiency across the flow rate regime, the reproducibility of the new nanoflow interface configuration was tested with replicate injections of 1 fmol BSA digest, as shown in Figure 3A. The chromatograms were qualitatively similar between injections, with an average CV of 3.95% for six replicate injections over the course of a 4 h time period. Figure 3B shows the microflow data for the same BSA sample. The equivalent injection of 1 µL (A) indicates approximately 3.5-fold reduction in the number of ions transmitted in microflow when compared to the data from 3A, while an injection of 10µL shows the expected 10-fold gain from the 1µL injection.

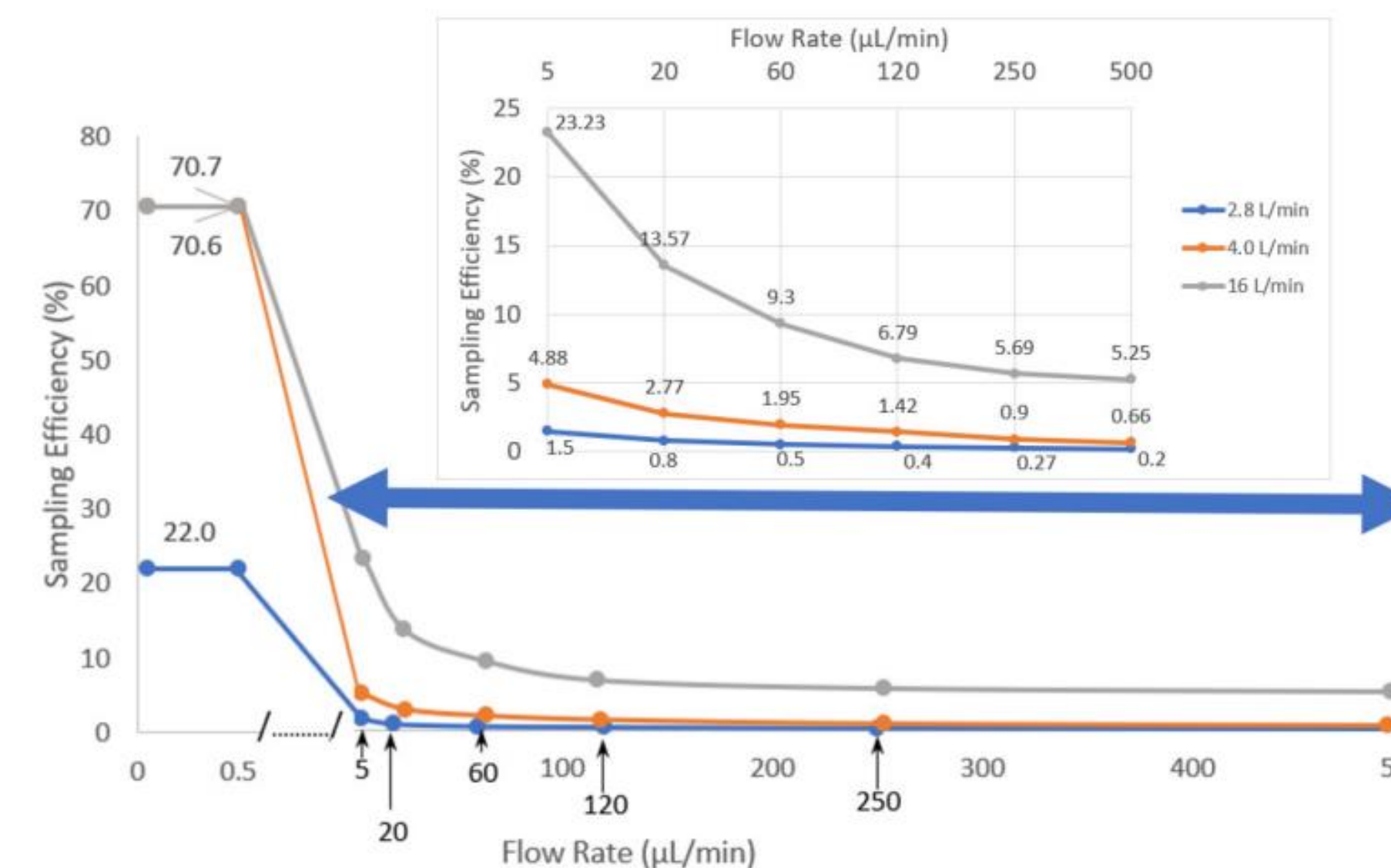


Figure 4. Electro spray sampling efficiency taken across 4 orders of magnitude flow rate. These data were taken using a mass spectrometer with approximately 4 L/min gas throughput (orange trace) and the prototype 16 L/min gas throughput configuration (gray trace), and the data points were added to the original plot taken on a system with 2.8 L/min gas throughput (blue trace) [4].

A series of six replicate injections were measured for each flow rate with either 4 or 16 L/min gas throughput, and the measured sampling efficiencies are plotted in Figure 4 along with the data taken a decade previously on a mass spectrometer with 2.8 L/min gas throughput. The results demonstrate a fundamental change in the shape of the sampling efficiency curve for the 16 L/min gas throughput configuration, and a general normalization of sampling efficiency across the flow range.

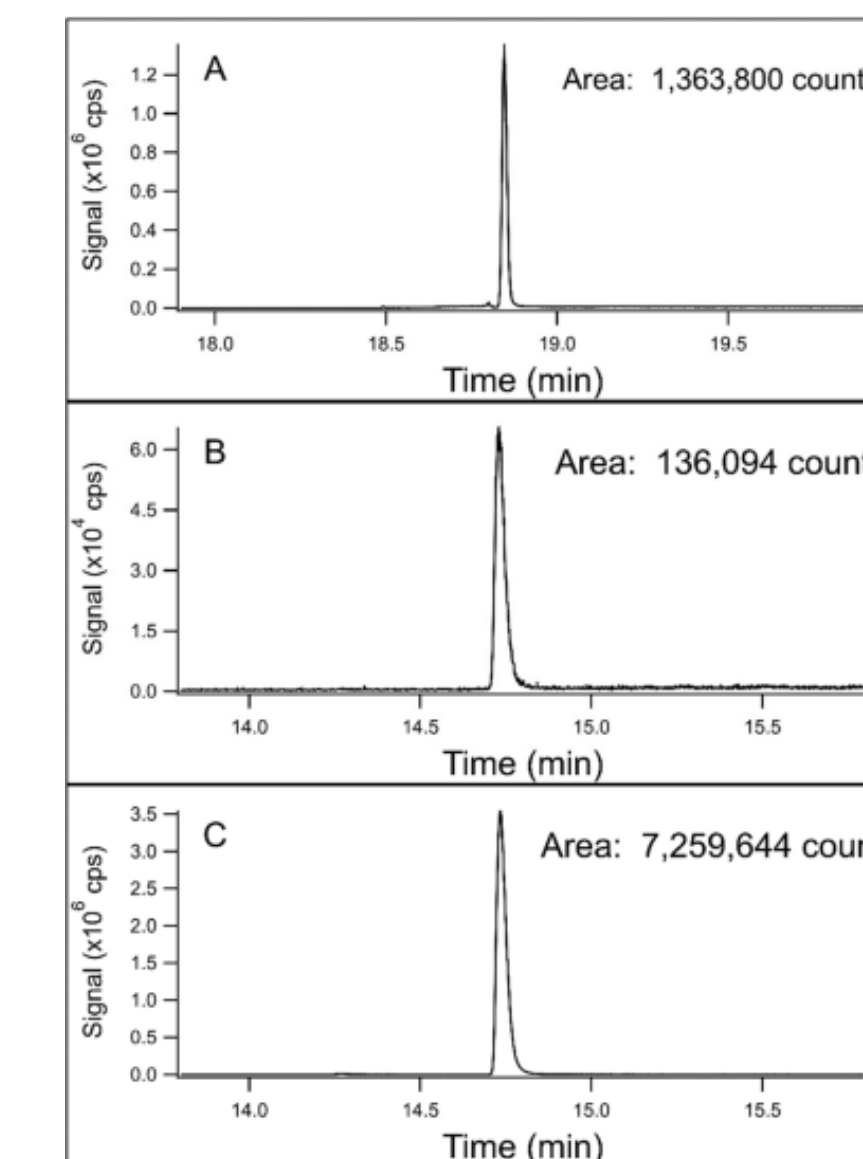


Figure 5. LC chromatograms for reserpine ions taken at 2 different ESI flow rates. (A) 1 µL injection with a nanoLC system at 300 nL/min, (B) 1 µL injection for a conventional LC-MS system operating at 300 µL/min, and (C) 50 µL injection for a conventional LC/MS system operating at 300 µL/min.

As expected from the sampling efficiency curve of Figure 4, the nanoflow LC-MS peak area was approximately 10-fold higher than the high flow peak area when injecting the same volume of sample. However, when accounting for the loading capacity advantage of the larger bore columns, it is possible to more than compensate for the difference in sampling efficiency. The theoretical difference in loading capacity for a 75 µm column vs a 2.1 mm column is 777X. For the data of Figure 5, pane C shows the high flow LC/MS data with a 50X greater injected volume, demonstrating no degradation of the peak.

CONCLUSIONS

The sampling efficiency of nanoflow ESI has achieved the theoretical limit of near 100%, and increasing the sampling inlet does not lead to further gains. The measured sampling efficiency difference between nanoflow ESI is approximately 3 × for microflow ESI and 13 × for milliflow ESI when using the highest sensitivity configuration. This represents a substantial improvement over previous interface configurations where the difference in sampling efficiency between the nanoflow and milliflow regimes was in excess of 100-fold. Calculations and experimental data are also provided to extrapolate the sampling efficiency differences into concentration detection limit differences between high flow and nanoflow ESI with this high gas load interface. In situations where sample is not limited to the extent that injection volumes approaching the capacity of the columns can be used, substantially lower concentration detection limits are expected to be achieved with the higher flow interfaces than with nanoflow ESI.

REFERENCES

- Schneider BB et. al., "Stable Gradient Nanoflow LC-MS", J. Am. Soc. Mass Spectrom., 2005, 16, 1545-1551.
- Javaheri H et. al., "Ion guide for Improved Atmosphere to Mass Spectrometer Vacuum Ion Transfer", J. Am. Soc. Mass Spectrom., 2021, 32, 1945-1951.
- Schneider BB et. al., "Particle Discriminator Interface for Nanoflow ESI-MS", J. Am. Soc. Mass Spectrom., 2003, 14, 1236-1246.
- Covey TR, et. al., "ESI, APCI, and MALDI A Comparison of the Central Analytical Figures of Merit: Sensitivity, Reproducibility, and Speed" *In Electrospray and MALDI Mass Spectrometry: Fundamentals, Practicalities, and Biological Applications*, 2nd ed.; Cole, RB Ed.; Wiley & Sons Inc.: New York, 2010; 443-485.

TRADEMARKS/LICENSING

The SCIEX clinical diagnostic portfolio is For In Vitro Diagnostic Use, Rx Only. Product(s) not available in all countries. For information on availability, please contact your local sales representative or refer to www.sciex.com/diagnostics. All other products are For Research Use Only. Not for use in Diagnostic Procedures.

Trademarks and/or registered trademarks mentioned herein, including associated logos, are the property of AB SCIEX Pte. Ltd. or their respective owners in the United States and/or certain other countries (see www.sciex.com/trademarks).